Acta Astronautica 205 (2023) 185–198

Contents lists available at ScienceDirect

Acta Astronautica

journal homepage: www.elsevier.com/locate/actaastro

Modeling and experimental assessment of *Synechococcus nidulans* cultivation using simulated Martian medium and astronauts' urine

Alessandro Concas [a,b,*], Giacomo Fais [b], Marco Enna [b], Susanna Zucchelli [b], Pierluigi Caboni [c], Nicola Lai [a], Alberto Cincotti [a], Giacomo Cao [a,b,c,d]

[a] Department of Mechanical, Chemical and Materials Engineering, University of Cagliari, Piazza D'Armi, 09123, Cagliari, Italy
[b] Interdepartmental Center of Environmental Science and Engineering (CINSA), University of Cagliari, Via San Giorgio 12, 09124, Cagliari, Italy
[c] Department of Life and Environmental Sciences, University of Cagliari, Via Ospedale 72, 09124, Cagliari, Italy
[d] Center for Advanced Studies, Research and Development in Sardinia (CRS4), Loc. Piscina Manna, Building 1, 09050, Pula, CA, Italy

ARTICLE INFO

Keywords:
Bio-ISRU
Synechococcus nidulans
Manned missions on mars
Algae
Cyanobacteria
Mathematical modeling

ABSTRACT

The growth of microalgae as food for astronauts is one of the main challenges in view of future manned missions on Mars. The possibility of cultivating the cyanobacterium Synechococcus nidulans in a medium consisting of a mixture of simulated regolith leachate and astronauts' urine, called Martian Medium, is investigated with the aim of reducing the payload deriving from nutrients to bring from Earth.

The strain was capable of surviving and grow with a biomass productivity of about 29 g m^{-3} day^{-1} in a medium containing 40% *v/v* of Martian Medium and urine. The composition of the strain, showing a prevalence of proteins, was not affected by the Martian Medium content up to 60% *v/v*. The produced biomass was characterized by a good antioxidant power and a relevant content of carotenoids that, together with the biochemical composition, make this strain a potential food for astronauts. The experimental results were well simulated by a mathematical model considering the effect of CO_2 level, light intensity, and Martian Medium content on the growth of the strain. Once validated, the model was used to predict the biomass productivities achievable when using Martian CO_2 in pressurized domes hosting the culture. The model estimated that a pond of about 85 m^2 and 40 cm deep hosted in CO_2 pressurized domes might allow to meet the 40% of proteins astronauts' needs during manned missions on Mars.

1. Introduction

It is nowadays widely acknowledged that issues such as Earth resources depletion, overpopulation, climate crisis, pandemics and wars, call for an immediate identification of suitable strategies to allow humanity to survive in the future. Though probably the most challenging, space colonization can be for sure considered among these possible strategies [1].

This goal can be pursued through the development of new technologies to sustain long duration manned missions in planets beyond the Lower Earth Orbit (LEO) [2]. These technologies should allow to produce *in-situ* consumables such as water, oxygen, and food [3–6]. Indeed, interplanetary trips are very expensive [7] and require consumables that cannot be continuously replenished from Earth. On the contrary, they should be produced with the available resources on the hosting planet according to a paradigm known with the acronym ISRU (*In Situ Resource Utilization*).

Among the planets where human life might be made possible by using this approach, Mars is one of the better candidates due to its proximity to Earth, which would allow even some re-supply trip, temperatures close to those of continental winters (−14 °C on average in the equator), day duration (~25 h), average solar irradiance levels (~20 E m^{-2} sol^{-1}) and resources availability such as atmospheric carbon dioxide (CO_2) water and regolith which might be transformed and exploited to produce useful consumables [8].

However, most ISRU technologies are based on physic-chemical methods for the production of oxygen and propellants but cannot contribute to the production of food [9,10]. Indeed, among the technologies to achieve such a goal, the ones relying on bio-engineering techniques that involve microalgae, macroalgae and cyanobacteria and fungi, can play a key role". It should be noted that only a few works dealt with the application of microorganisms to transform *in-situ*

* Corresponding author. Department of Mechanical, Chemical and Materials Engineering, University of Cagliari, Piazza D'Armi, 09123, Cagliari, Italy.
E-mail address: alessandro.concas@unica.it (A. Concas).

https://doi.org/10.1016/j.actaastro.2023.01.027
Received 12 March 2022; Received in revised form 22 December 2022; Accepted 19 January 2023
Available online 31 January 2023

resources available on Mars into food. The so called bioregenerative ECLSSs (Environmental Control Life Support Systems) takes into account the production of food by recycling cabin air and metabolic wastes [2,3,6,11]. However, the amount produced is not sufficient to supply the daily caloric needs of a crew, which have been estimated to be ~3000 cal sol^{-1} per component of the crew [8]. Thus, biobased ISRU technologies for food production on Mars are needed.

Two main categories of bio-ISRU technologies can be used to this aim, i.e., the ones relying on methylotrophic bacteria and autotrophic microorganisms, respectively. The first ones consist of using methanol, which can be produced *in-situ* via physic-chemical ISRU [9], to obtain protein-rich edible biomass by means microorganisms such as *Pichia pastoris* and *Methylophilus methyloprophus* or engineered *Escherichia coli* and *Bacillus subtilis* [8,12]. The second category of bio-ISRU processes are based on rock weathering cyanobacteria which photosynthetically convert nitrogen (N_2) and CO_2 available in the Mars atmosphere, along with sulfur (S), phosphorus (P), iron (Fe) and several micronutrients which can be extracted from the regolith, into newly formed edible biomass by relying on the water and light available *in-situ* [11,13]. The use of cyanobacteria and microalgae leads to the further positive effect of producing photosynthetic oxygen crucial for the crew and to integrate the corresponding amount produced via physic-chemical methods.

The possibility of using several cyanobacteria, exposed to simulated Martian conditions (−27 °C, 0.8 kPa, pure CO_2) has been investigated by Olsson-Francis and Cockell [13] who found that the strains *A. cylindrica*, *Chroococcidiopsis 029*, *Gloeocapsa OU_20*, *Phormidium OU_10* and *Leptolyngbya OU_13* were able to survive several days using a regolith simulant as growth substrate [13].

Recently Verseux et al. [11] investigated the diazotrophic growth of *Anabaena* sp. PC7983 under an artificial low-pressure (~101 hPa) atmosphere composed by N_2 (96%) and CO_2 (4%) which the authors envisioned to be produced by taking advantage of the Martian atmosphere. This strain was capable to grow by taking up C and N from such atmosphere and other micronutrients from a Martian regolith simulant immersed in the growth medium BG-11 [11]. Thus, whereas the possibility to produce these conditions within closed domes on Mars still needs to be evaluated, this work demonstrated that cyanobacteria cultivation by exploiting *in-situ* available resource on Mars might be feasible.

A study where Mars-like conditions are taken into account [14] investigated the capability of the autotrophic strain *Chrococcidiopsis* sp. CCMEE 029 to tolerate perchlorate salts, that are typically found in Mars regolith. The results showed that the growth of this strain was not affected by Mars-relevant concentrations of Magnesium (Mg) or Calcium (Ca) perchlorate, thus demonstrating that *Chrococidiopsis* is a good candidate for bio-ISRU contexts on Mars.

. Although great efforts are being made to develop novel techniques to cultivate microalgae on Mars, further research activity is needed to verify the possibility to use microalgae and cyanobacteria as potential food source in the framework of manned missions on Mars that rely on ISRU technologies. Accordingly, in this work, we investigate the possibility of using a mixture of simulated Mars regolith leachate and astronaut's urine to grow the cyanobacterium called *Synechococcus nidulans*. To be used as potential food by the crew members. We chose to investigate *Synechococcus nidulans* because it is an extremophile cyanobacterium capable of adapting to extreme environments such the ones taking place on Mars. While urine could supply macronutrients such as phosphates and ammonium, regolith leachate could provide relevant micronutrients and in particular iron which is known to strongly affect the growth microalgae and cyanobacteria [15]. Also, the nutritional characteristics of the biomass produced using the above growth media are investigated for the first time. The experimental results have been interpreted by a mathematical model that allows the identification of the set of operating conditions to maximize the biomass, and thus food productivity.

The results of this activity provide a first assessment on the possibility of growing this strain within a pressurized and heated dome on Mars, in the framework of the general ISRU-ECLSS process recently proposed by Cao et al. [16] in the patent literature. This process involves two interacting sections, i.e., the physic-chemical one and the biological one. In the first section, different units specifically designed to operate under Martian conditions, permit to produce water, oxygen, and propellants along with suitable amounts of fertilizers to be used in biological section. The biological section takes as inputs local natural resources (CO_2 from atmosphere and regolith), urine from the ECLSS and the outputs from the physic-chemical allowing to produce edible biomass and photosynthetic oxygen by growing microalgae and or cyanobacteria in photobioreactors hosted by pressurized and heated domes.

2. Materials and methods

2.1. Microorganism maintenance

Unialgal culture of cyanobacterium *Synechococcus nidulans* CCALA 188 was obtained from the Culture Collection of Autotrophic Organisms (CCALA) in Třeboň, Czech Republic. The strain was maintained under axenic conditions. The cultures were kept in 250 mL Erlenmeyer flask, containing 150 mL Z-medium (Table 1). Prior to inoculation, the flasks containing the culture media were autoclaved at 121 °C for 15 min. The cultures were kept under photoautotrophic conditions and incubated in a thermostatically controlled chamber at 20 ± 1 °C. The photoperiod was fixed at 12:12 h light and dark periods with white light illumination of 25 μmol m^{-2} s^{-1} (Lightmeter Delta OHM HD 2302.0). The use of the photoperiod was necessary to permit the dark phase reactions of photosynthesis to take place, Stirring was set at 100 rpm.

2.2. Preparation and composition of the Martian medium (MM)

Synthetic Martian Medium (MM) was prepared by mixing a leachate of Martian regolith simulant (JSC MARS-1) and synthetic human urine (MP-AU) to simulate astronauts' urine. Main constituents of JSC MARS-1 used in the present study were reported in Table 2 in terms of oxides wt %.

According to the literature [17], the mineral phases of JSC MARS-1 identified by XRD analysis consisted primarily of tectosilicate plagioclase feldspar, pyroxene, iron oxides (magnetite and hematite), ilmenite and olivine.

The regolith leachate (RL) was prepared within a 250 mL Erlenmeyer

Table 1
Composition of Z-medium.

Macronutrients	mg L^{-1}
$NaNO_3$	467.0
$Ca(NO_3)_2{\cdot}4H_2O$	59.0
K_2HPO_4	31.0
$MgSO_4{\cdot}7H_2O$	25.0
Na_2CO_3	21.0
$FeCl_3{\cdot}6H_2O$	3.6
Na_2EDTA	3.7
Trace elements	**μg L^{-1}**
H_3BO_3	248.0
$MnSO_4{\cdot}4H_2O$	178.4
$Na_2WO_4{\cdot}2H_2O$	2.4
$(NH_4)6Mo_7O_{24}{\cdot}4H_2O$	7.0
KBr	9.5
KI	6.6
$ZnSO_4{\cdot}7H_2O$	22.9
$Cd(NO_3)_2{\cdot}4H_2O$	12.3
$Co(NO_3)_2{\cdot}6H_2O$	11.7
$CuSO_4{\cdot}5H_2O$	10.0
$NiSO_4(NH_4)\ 2SO_4{\cdot}6H_2O$	15.8
$Cr(NO_3)_2{\cdot}7H_2O$	2.9
$V_2O_4(SO_4)_3{\cdot}16H_2O$	2.8
$Al_2(SO_4)\ 3K_2SO_4{\cdot}24H_2O$	37.9

Table 2
Fractional percentage of oxides in the Martian Regolith simulant JSC Mars-1A.

Major element composition[a]	wt %
Silicon dioxide (SiO_2)	34.5–44.0
Titanium dioxide (TiO_2)	3.0–4.0
Aluminum oxide (Al_2O_3)	18.5–23.5
Ferric oxide (Fe_2O_3)	9.0–12.0
Iron oxide (FeO)	2.5–3.5
Magnesium oxide (MgO)	2.5–3.5
Calcium oxide (CaO)	5.0–6.0
Sodium oxide (Na_2O)	2.0–2.5
Potassium oxide (K_2O)	0.5–0.6
Manganese oxide (MnO)	0.2–0.3
Diphosphorus pentoxide (P_2O_5)	0.7–0.9

[a] The normal convention for data presentation uses oxide formulae from an assumed oxidation state for each element (with the exception of Fe) and oxygen is calculated by stoichiometry.

flask with a cap by contacting 15 g of regolith simulant (<1 mm diameter size) with 150 mL of ultrapure water (pH 6.80). The solid liquid mixture was stirred at 200 rpm with an orbital shaker (Stuart SSM1, Bio sigma) for 24 h at 25 °C. Then the solution was filtered by gravity by means of filter paper.

Analysis of the supernatant was carried out using an inductively coupled plasma (ICP) optical emission spectrometry (Varian 710-ES ICP OES) for the determination of aluminum (Al), calcium (Ca), iron (Fe), potassium (K), magnesium (Mg), manganese (Mn), sodium (Na), phosphorus (P), silicon (Si), and (titanium) Ti. The ICP was operated under the following conditions: radiofrequency generator power 1.2 kW, frequency 40 MHz; Ar (99.996% purity) was used both for plasma (15 L/min), nebulizer (200 Kpa), and optic supply (1.5 L/min), respectively. The spray chamber was a double-pass, glass cyclonic. The power and pressure applied were 600 W and 100 PSI, respectively for 13 min. Calibration curves were elaborated on five points and considered acceptable for $R^2 \geq 0.999$. The results of RL analysis through ICP are shown in Table 3.

Synthetic human urine (MP-AU) was produced according to available protocols [18] and then diluted with ultrapure water at a ratio of 1:10 to both simulate the corresponding effect of flushing water in ECLSS systems and meet the nitrogen requirement of microalgae. The chemical composition of diluted human urine simulant is shown in Table 4.

Finally, the leachate of Martian regolith and diluted urine were mixed (1:1 *v:v*) to produce the so-called Martian Medium (MM). Conductivity was 850 μS/cm and pH 7.4 at 25 °C. Dilutions of MM (20, 40, 60 and 80%) were made whit Zarrouk's medium which was also the experimental control medium. MM and its dilutions have been sterilized at 121 °C for 15 min prior to use. Table 5 shows the macronutrient and metal concentrations in the Martian Medium. Some of the metals, such as Zn, Fe, Mg, Si, Mn, and K, served as micronutrients for cyanobacteria.

The experiments were then performed using different culture media

Table 3
Heavy Metals and micronutrients in the Martian Regolith leachate (RL).

Metal	mg L^{-1}
Al	4.80
Ca	8.12
Fe	6.41
K	8.32
Mg	1.48
Mn	0.19
Na	4.66
P	0.25
Si	10.28
Ti	1.27

Table 4
The composition of synthetic urine (MP-AU)[a].

Components	g L^{-1}
Na_2SO_4	1.70
$C_5H_4N_4O_3$	2.50
$Na_3C_6H_5O_7{\cdot}2H_2O$	0.72
$C_4H_7N_3O$	0.88
CH_4N_2O	15.00
KCl	2.30
NaCl	1.75
$CaCl_2$	0.18
NH_4Cl	1.26
$K_2C_2O_4{\cdot}H_2O$	0.03
$MgSO_4{\cdot}7H_2O$	1.08
$NaH_2PO_4{\cdot}2H_2O$	2.91
$Na_2HPO_4{\cdot}2H_2O$	0.83

[a] $C_5H_4N_4O_3$ = huric acid; $Na_3C_6H_5O_7{\cdot}2H_2O$ = Sodium citrate dihydrate; $C_4H_7N_3O$ = Creatinine; CH_4N_2O = Urea.

Table 5
The concentration of macro-nutrients and metals acting as micronutrients in the Martian Medium (MM).

Macronutrient	mg L^{-1}
Na_2SO_4	85
$C_5H_4N_4O_3$	12
$Na_3C_6H_5O_7{\cdot}2H_2O$	36
$C_4H_7N_3O$	44
CH_4N_2O	750
KCl	115
NaCl	87
$CaCl_2$	9
NH_4Cl	63
$K_2C_2O_4{\cdot}H_2O$	2
$MgSO_4{\cdot}7H_2O$	54
$NaH_2PO_4{\cdot}2H_2O$	146
$Na_2HPO_4{\cdot}2H_2O$	41
Trace elements	**μg L^{-1}**
Al	945
Ca	4595
Fe	1305
K	4655
Mg	790
Mn	3
Na	370
P	9
Si	368
Ti	25

composition obtained by replacing specific volumes of Z-medium with equal volumes of Martian Medium. The resulting composition of the media, hereafter named with the suffix MM followed by the volume percentage of Z-medium replaced with Martian medium, is reported in Table 6.

2.3. Growth experiments to optimize MM content in the culture medium

Growth experiments were performed using media consisting of mixtures of MM and Z-medium wherein the volume percentages of MM were equal to 0, 20, 40 and 60%, respectively. The batch culture experiments were carried out within 75 cm^3 rectangular transparent vented cap flasks filled up to 40 mL (Corning™). The experiment was set in triplicates with an illumination of 100 μE m^{-2} s^{-1} on the irradiated surface of the culture flask. The optical density at the beginning of the experiments was about 0.2 at a wavelength of 650 nm. Before inoculating the cells, morphology was examined using magnification of 40 and 100 X (Leica DM750) optical microscope interfaced with Leica EC3 digital camera (Leica Microsystems, Wetzlar, Germany), and the Leica Application Suite (version 3.4.0, Leica Microsystems). All operations

Table 6
IDs and composition of the media.

Medium name	MM-60	MM-40	MM-20
Volume of Martian medium	60 %v/v	40 %v/v	20 %v/v
Major elements	mg L^{-1}	mg L^{-1}	mg L^{-1}
Na_2SO_4	51.0	34.0	17.0
$C_5H_4N_4O_3$	7.5	5.0	2.5
$Na_3C_6H_5O_7{\cdot}2H_2O$	21.6	14.4	7.2
$C_4H_7N_3O$	26.4	17.6	8.8
CH_4N_2O	450.0	300.0	150.0
KCl	69.2	46.2	23.1
NaCl	52.7	35.1	17.6
$CaCl_2$	5.6	3.7	1.9
NH_4Cl	38.0	25.3	12.7
$K_2C_2O_4{\cdot}H_2O$	1.1	0.7	0.4
$MgSO_4{\cdot}7H_2O$	32.5	21.6	10.8
$NaH_2PO_4{\cdot}2H_2O$	87.4	58.2	29.1
$Na_2HPO_4{\cdot}2H_2O$	24.9	16.6	8.3
$NaNO_3$	186.8	280.2	373.6
$Ca(NO_3)2{\cdot}4H_2O$	23.6	35.4	47.2
K_2HPO_4	12.4	18.6	24.8
$MgSO_4{\cdot}7H_2O$	10.0	15.0	20.0
Na_2CO_3	8.4	12.6	16.8
$FeCl_3{\cdot}6H_2O$	1.4	2.2	2.9
Na_2EDTA	1.5	2.2	3.0
Trace elements	**μg L^{-1}**	**μg L^{-1}**	**μg L^{-1}**
H_3BO_3	100.0	150.0	200.0
$MnSO_4{\cdot}4H_2O$	72.0	108.0	144.0
$Na_2WO_4{\cdot}2H_2O$	1.0	1.4	1.9
$(NH_4)_6Mo_7O_{24}{\cdot}4H_2O$	2.8	4.2	5.6
KBr	3.8	5.7	7.6
KI	2.6	4.0	5.3
$ZnSO_4$ x $7H_2O$	9.2	13.8	18.4
$Cd(NO_3)_2{\cdot}4H_2O$	4.8	7.2	9.6
$Co(NO_3)_2{\cdot}6H_2O$	4.8	7.2	9.6
$CuSO_4{\cdot}5H_2O$	4.0	6.0	8.0
$NiSO_4(NH_4)_2SO_4{\cdot}6H_2O$	4.8	7.2	9.6
$Cr(NO_3)_2{\cdot}7H_2O$	1.2	1.8	2.4
$V_2O_4(SO_4)_3{\cdot}16H_2O$	1.1	1.7	2.2
$Al_2(SO_4)_3K_2SO_4{\cdot}24H_2O$	15.2	22.8	30.4

were carried out under a microbiological safety cabinet to avoid environmental contamination. The growth was monitored through absorbance spectrophotometric measurements (Genesys 20 spectrophotometer, Thermo Scientific, Walthmanm Waltham, USA) of the chlorophyll-a optical density (OD) of the culture at 650 nm wavelength. The biomass concentration C_x (g L^{-1}) was calculated from OD measurements using the calibration curve C_x vs OD shown in Fig. 1.

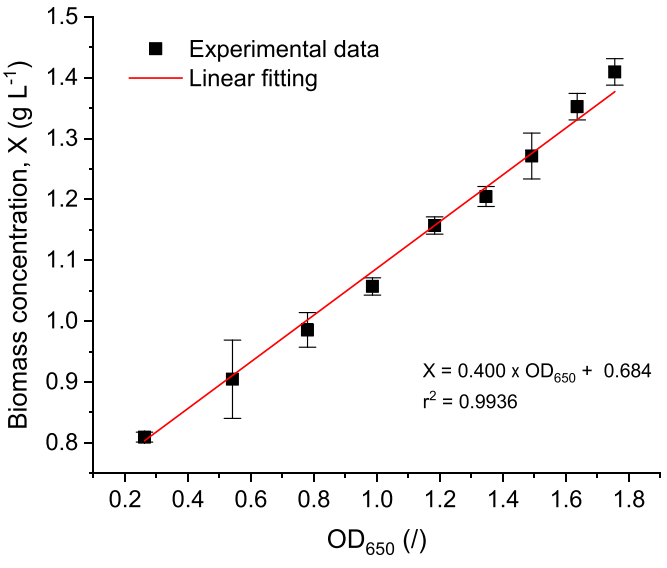

Fig. 1. Calibration line X Vs OD for *Synechococcus nidulans*.

The calibration was obtained by gravimetrically analysis of the biomass concentration of known culture volumes previously centrifuged at 4000 rpm for 15 min and dried at 105 °C for 24 h. The pH was measured daily by pH-meter (Basic 20, Crison).

2.4. Biomass characterization

2.4.1. Reagents and standards

Methanol and chloroform were grade RPE-ACS-for analysis -Reag. Ph. Eur.-Reag and were purchased from Sigma-Aldrich (Merck KGaA, Darmstadt, Germany). Sulfuric acid 96%, orthophosphoric acid 85%, sodium nitrate, potassium chloride, phenol, copper sulphate, sodium hydroxide, and sodium potassium tartrate were grade RPE-ACS-for analysis-reag. Ph. eur.-reag and were purchased from Carlo Erba (Val de Reuil Cedex, France). Sodium carbonate and Folin-Ciocalteau reagent were acquired by Sigma-Aldrich Inc. (St. Louis, MO, USA). Glucose, bovine serum albumin and vanillin standards were acquired by Sigma-Aldrich (Merck Kgaa, Darmstadt, Germany). Ultrapure water with conductivity below 18.2 MΩ was obtained by distillation with a Milli-Q system (Millipore, Bedford, MA, USA).

2.4.2. Preparation of freeze-drying sample powder

An aliquot of *Synechococcus* culture was centrifuged at 4000 rpm for 10 min at 20 °C. The supernatant was discarded, the pellet was resuspended in Milli-Q water and the washing procedure was repeated three-times. The cellular pellet was frozen at −80 °C, lyophilized with LIO-5PDGT freeze-dryer (5 Pa, Milano, Italy) and suitably pulverized with mortar. The dried powder was stored in darkness inside a glass vacuum desiccator before analytical purposes.

2.4.3. Total carbohydrates, lipids, and soluble proteins

The determination of total carbohydrates was carried out according to the suitably modified method proposed by Dubois et al. [19]. 2 mg of freeze-dried biomass were weighed inside an Eppendorf tube and suspended in 1000 μl of phosphate-buffered saline (PBS) (20 mM, pH 7.4). Approximately 150 mg of 1–1.3 mm glass balls were added, the samples were vortexed for 10 min and sonicated in an ultrasonic bath for 10 min at 20 °C for three times. 200 μl of the extract was transferred to a glass tube while 200 μl of phenol 5% (w/v) and 1000 μl of concentrated sulfuric acid were added. The samples were filtered with 0.45 μm PTFE membrane filter and analyzed at $\lambda = 490$ nm using a Varian Cary 50 spectrophotometer. The quantitative analysis was carried out by the external standard method using glucose as reference species.

The 5-points calibration line was made by correlating the absorbance with the glucose concentration. The results were reported as means ± standard deviation and expressed in mg/kg of glucose. All samples were analyzed in triplicate.

The determination of total lipids was carried out according to the protocol indicated by Chen et al. [20] with minor changes as follows. The 100 μl of PBS, 1,5 mL of 25% methanol, and 1 N sodium hydroxide solution were added to 2 mg of lyophilized sample. The suspension was sonicated for 10 min in an ultrasonic bath and then heated to 100 °C for 30 min. Lipids were then extracted using the method proposed by Bligh and Dyer [21]. The colorimetric reaction was carried out according to the method proposed by Mishra et al. [22]. All samples were analyzed in triplicate and the results were expressed in mg/kg± SD.

The determination of protein content was carried out according to the method by Lowry et al. [23]. Briefly, 1000 μl of PBS, 20 mM, pH 7.4, was added to 2 mg of lyophilized sample. Approximately 150 mg of 1–1.3 mm glass balls were added and vortexed for 10 min and sonicated in an ultrasonic bath for 10 min at 20 °C for three times. 250 μl of this solution reacted with 250 μl of 1 N sodium hydroxide for 5 min at 100 °C. After cooling for 10 min, 2,5 mL of a 5% sodium carbonate (w/v), 0,5% (w/v) cupric sulphate and 1% (w/v) sodium potassium tartrate solution were added to the sample. After 10 min, 0,5 mL of 1 N

Folin-Ciocalteau reagent was also added. Samples were analyzed at λ = 750 nm with a spectrophotometer (Varian Cary 50). The quantitative analysis was carried out using the external standard method by correlating the absorbance (Abs) with the concentration of bovine serum albumin (BSA) solutions. All samples were analyzed in triplicate and the results were expressed in mg/kg ± SD of BSA.

2.4.4. Antioxidant activity

The DDPH spectrophotometric assay was performed in accordance with the method by Brand-Williams et al. [24]. Briefly, 250 μl of methanol were added to 2 mg of lyophilized *Synechococcus* powder. Approximately 100 mg of 1–1.3 mm glass balls were then added, and the solution was vortexed for 10 min and sonicated in an ultrasonic bath for 10 min at 10 °C for three times. The sample was centrifuged for 5 min at 4000 rpm 50 μl of the methanol extract supernatant was added to 2 mL of a methanol solution of DDPH (50 μmol) for the determination of total or standard polyphenols (Trolox). After 60 min of incubation the solutions were analyzed at λ = 517 nm. The quantitative analysis was carried out using the external standard method (Trolox) correlating the absorbance with the concentration. The results were expressed in mmol/kg TEAC (Trolox equivalent antioxidant capacity).

2.4.5. Chlorophyll-a and total carotenoids content

The method proposed by Zavrel et al. [25] was adopted. Briefly, 1000 μl of culture were placed inside Eppendorf tubes and centrifuged at 10,000 rpm for 10 min at 4 °C. The supernatants were discarded, and 1 mL of neutralized methanol was added to the pellets. The solutions were left one night in the fridge and after 24 h, approximately 150 mg of 1–1.3 mm glass balls were added. The samples were homogenized using three cycles of 10 min of a vortex and ultrasonic bath. The solutions were centrifuged for 10 min at 10,000 rpm. Spectrophotometric analysis was performed on the supernatant for chlorophyll-a and total carotenoids at λ = 720 nm, λ = 665 nm, respectively while λ = 470 nm was used for methanol as a blank. The following correlations proposed by Ricthie [26] and Wellburn [27], were used to estimate the total carotenoids and chlorophyll-a concentrations, respectively:

$$Chl-a\left[\mu g\ ml^{-1}\right]=12.9447\ (A_{665}-A_{720})$$

$$Carotenoids\left[\mu g\,mL^{-1}\right]=\left(1000\,(A_{470}-A_{720})-2.86\left(Chl-a\left[\mu g\,mL^{-1}\right]\right)\right)/221$$

3. Mathematical model

The experimental data have been simulated by a mathematical model of chemical reactions taking place in stirred tanks operated in a semi-batch mode, i.e., batch for the liquid and continuous for the gaseous phase, respectively. Thus, the model accounts for the diffusive mass transfer of CO_2 between the gas and the liquid phase with the culture. Specific nutrient's concentration, light intensity, and medium pH, respectively, were the main limiting growth factors. The dynamic mass balance equation for the functional microalgal biomass may be reported as follows [28,29]:

$$\frac{dX}{dt}=\mu_{\max}\cdot f(\mathbf{N})\cdot g(I_{av})\cdot h(pH)\cdot X-\mu_d\cdot X \tag{1}$$

along with the initial condition:

$$X=X^0\ \ @\ \ t=0 \tag{2}$$

Symbol's significance is reported in the notations. The terms $f(\mathbf{N})$, $g(I_{av})$ and $h(pH)$ are suitable functions expressing the growth-limiting effect of nutrients **N**, average photosynthetically active photon flux within the culture I_{av}, and pH, respectively. Among the macronutrients, total inorganic carbon (TIC), nitrogen (TIN) and phosphorus (TIP) were assumed to be limiting. The Monod's kinetics was adopted for all macronutrients to describe their influence on microalgae growth rate:

$$f(\mathbf{N})=\prod_{j=1}^{n}\frac{[C_j]}{[C_j]+K_j}\quad \text{where}\quad j=TIC,TIN,TIP \tag{3}$$

Moreover, according to the literature, the kinetic dependence of growth rate on light intensity, $g(I_{av})$ was evaluated as follows [30]:

$$g(I_{av})=\frac{I_{av}}{I_{av}+I_{K,h}+\frac{I_{av}^2}{I_{K,i}}} \tag{4}$$

where the average light intensity $I_{av}(\mu E\,m^{-2}s^{-1})$, within a rectangular culture flask, was calculated according to Grima et al. [31] through the following equation:

$$I_{av}(t)=\frac{I_0(t)}{L\cdot\tau_a\cdot X}\left[1-\exp(-L\cdot\tau_a\cdot X)\right] \tag{5}$$

where L is the length of the rectangular basis in the direction parallel to the light beam. Since microalgae enzymes contain ionizable functional groups which, depending on pH, present different specific ionization states, microalgae growth rate can be strongly influenced by culture pH [32]. To describe the dependence of μ on pH, the model proposed by Tan et al. [33], was adopted:

$$h(pH)=h([H^+])=\left(\frac{\frac{k_0}{k_1}+\frac{1}{K_1}[H^+]+\frac{k_2}{k_1K_1K_2}[H^+]^2}{1+\frac{1}{K_1}[H^+]+\frac{1}{K_1K_2}[H^+]^2}\right) \tag{6}$$

In the liquid phase, the total inorganic carbon (TIC) concentration change was described by a mass balance which considers carbon consumption by microalgae and CO_2 mass transfer to the gas phase:

$$V_L\frac{d[CTIC]}{dt}=V_Rk_La\left(H_{CO_2}\left[C_{g,CO_2}\right]-\left[C_{L,CO_2}\right]\right)-Y_{TIC}\frac{dX}{dt}V_L \tag{7}$$

along with the initial condition:

$$[C_{TIC}]=\left[C_{TIC}^0\right]\ \ @\ \ t=0 \tag{8}$$

The CO_2 concentration in the gas phase (C_{g,CO_2}) was related to the molar fraction of CO_2 in air (x_{CO_2}) by the ideal gas law as:

$$\left[C_{g,CO_2}\right]=\left[C_{g,CO_2}^0\right]=x_{CO_2}\frac{P_{air}}{RT}\,\text{for}\forall t \tag{9}$$

Once adsorbed in the liquid phase, CO_2, which is assumed to be in equilibrium with the gas phase, contributes to alter the speciation equilibria reported in Table 7.

Based on the mass action law of equilibria (E1- E4) and the equation expressing the electroneutrality, as well as on the calculations reported in Appendix 1, it is possible to express $[H^+]$ as a function of the concentration of total inorganic carbon and equilibrium constants as reported in what follows.

$$[H^+]=\frac{K_W}{[H^+]}+K_{1C}K_C\frac{[H^+][C_{TIC}]}{\psi([H^+])}+2K_{2C}K_{1C}K_C\frac{[C_{TIC}]}{\psi([H^+])}+[Alk] \tag{10}$$

The only unknown $[H^+]$ was evaluated by numerical methods once the instantaneous value of C_{TIC} is available. The term $[Alk]$ in Eq. (10)

Table 7
Equilibrium and corresponding constants of the main reactions involving carbon species in the liquid phase.

ID	Chemical Equilibrium	pK	Ref.
E 1	$CO_{2L}+H_2O\overset{K_C}{\rightleftarrows}H_2CO_3$	2.77	[34]
E 2	$CO_{2L}+OH^-\overset{K_C}{\rightleftarrows}HCO_3^-$	6.32	[35]
E 3	$H_2CO_3\overset{K_{1C}}{\rightleftarrows}H^++HCO_3^-$	3.6	[36]
E 4	$HCO_3^-\overset{K_{2C}}{\rightleftarrows}H^++CO_3^{2-}$	10.33	[36]

represents the summation of non-carbonic ions species concentrations in the electro-neutrality condition as shown in Eq. (A10) of Appendix 1.

According to the considerations made in Appendix 1, the non-carbonic alkalinity [*Alk*] varies in time because of ions uptake by microalgae and its evolution was described by the equation:

$$\frac{d[Alk]}{dt} = Y_{Alk}\frac{dX}{dt} \tag{11}$$

which can be solved along with the initial condition

$$[Alk] = [Alk^0] @ t = 0 \tag{12}$$

where $[Alk^0]$ was calculated imposing the known initial values $[H^+] = [H^+]^0$ and $[C_{TIC}] = [C^0_{TIC}]$ in Eq. (10). The mass balance for the limiting nutrients TIN and TIP in the liquid phase was defined as:

$$\frac{d[C_J]}{dt} = -Y_J\frac{dX}{dt}\cdot\theta(I_{av}) \quad \text{with} \quad J = TIN, TIP \tag{13}$$

along with the corresponding initial conditions:

$$[C_J] = [C_J^0] \quad \text{with} \quad J = TIN, TIP \tag{14}$$

The variable $\theta(I_{av})$ considered that in absence of light there was neither consumption nor production of nutrients and was defined as follows:

$$\theta(I_{av}) = \begin{cases} 1 & \text{when } I_{av} > 0 \\ 0 & \text{when } I_{av} \leq 0 \end{cases} \tag{15}$$

The resulting system of ODEs constituted by Eqs ((1), (7), (11) and (13) was then solved along with the non-linear algebraic Eq. (10). Differential equations were numerically integrated as an initial value problem using the subroutine DIVPAG of the standard numerical libraries (IMSL) that implements the fifth-order Gear's backward differentiation formulae in Fortran 90 (Compaq Visual Fortran 6.1). The nonlinear Eq. (10) was solved using the IMSL subroutine DZBREN (Compaq Visual Fortran 6.1) which implements numerical algorithm based on the combination of linear interpolation, inverse quadratic interpolation, and bisection. Some model parameters were taken from the literature while some others were suitably tuned by fitting the experimental data through the Fortran subroutine BURENL [35]. In this subroutine the objective function is evaluated as the weighted sum of the objective functions related to pH and biomass concentration data. Each of the two functions consisted of the sum of square errors of the model with respect to experimental data. The minimum of the resulting objective function is searched through the golden section algorithm.

4. Results and discussion

The time profile of the biomass concentration and pH during these experiments are shown in Fig. 2.

By starting from an initial concentration of 0.8 g L^{-1} the strain was capable of achieving a concentration of about 1.2 g L^{-1} after ten days of cultivation in pure Z-medium (cf. Fig. 2a). It should be noted that growth took place albeit a low PPFD of just 20 μE m^{-2} s^{-1} was provided to the cultures and atmospheric CO_2 diffusion occurred passively through the permeable membrane in the vented cap rather than through CO_2 bubbling. The medium's pH increased correspondingly from 8 to about 10.5 because of the photosynthetic activity of algae utilized the dissolved CO_2 and bicarbonates during their growth.

To simulate this experiment, the model parameters in Eq. (6) were estimated by a fitting procedure using the experimental data by De

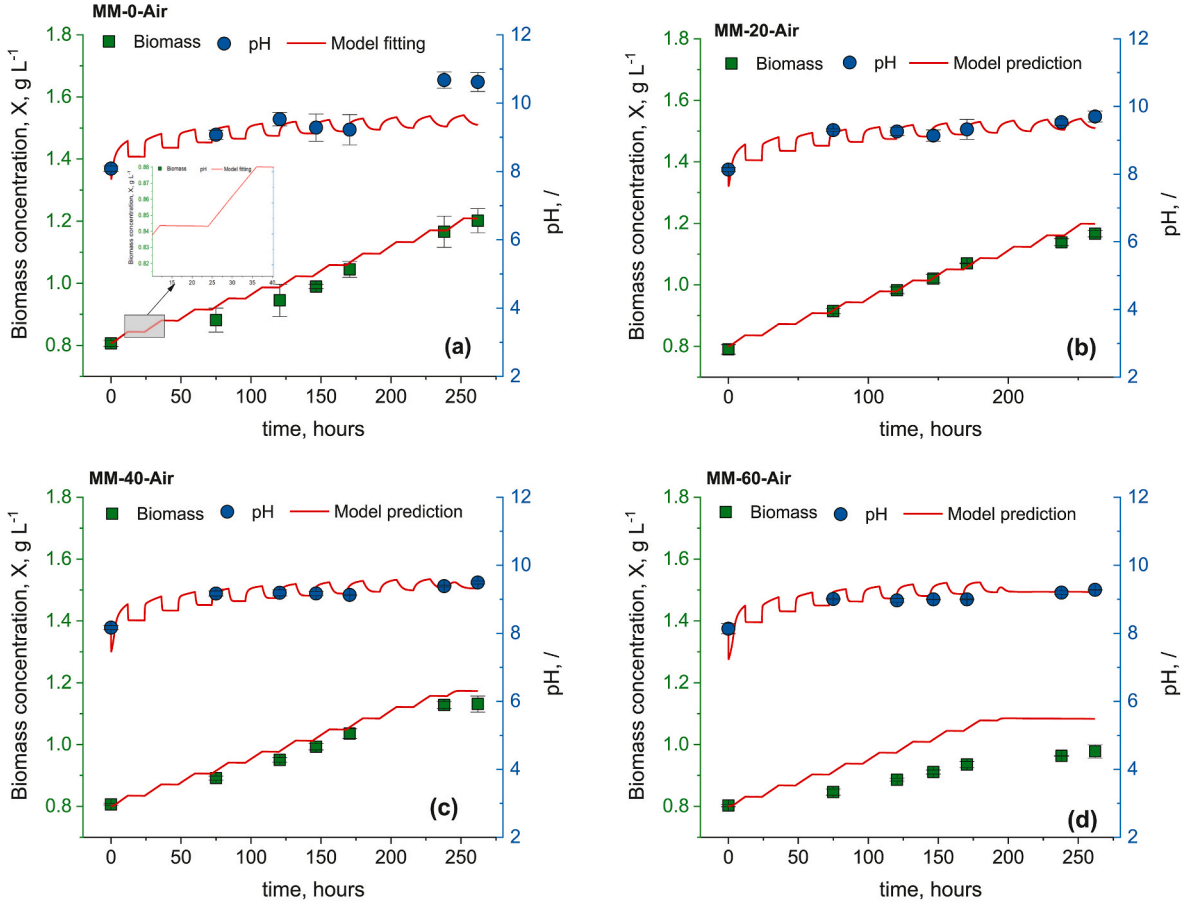

Fig. 2. Effect of volume replacements of Z-Medium with equal volumes of Martian Medium MM (a) 0%, (b) 20%, (c) 40%, (d) 60%.

Farias Silva et al. [37] reported in Fig. 3. In the same Figure, it is also shown the effect of pH on the $h(pH)$ for the strain *Synechococcus* PCC 7002.

The best fitting values for these parameters are reported in Table 8. It should be noted that, while few pH values were evaluated in the investigation by De Farias Silva et al. [37], the latter represents the only study in the literature capable to provide an experimental evaluation of $h(pH)$ for the concerned strain.

Once the parameters in Eq (6) are obtained, the time evolution of biomass concentration and pH reported in Fig. 2a were simulated by using the literature values of model parameters along with the tuned values of Y_{TIP} and Y_{Alk} reported in Table 9. The latter ones represent the TIP and non-carbonic alkalinity (Alk) consumed per unit weight of biomass produced, respectively, and, while the obtained value of the former one was close to corresponding literature values of other strains [28]. Even the value of Y_{Alk} was consistent with the one provided in the literature [28]

Fig. 2a shows that the experimental data are well simulated by the proposed model when tuning only two parameters against two series of data. Indeed, an average relative error equal to 3.53% and an adjusted r^2 value of 0.997 were obtained through the fitting procedure. As far model results, it is worth mentioning that the seemingly wavering trend of model results depends on that a photoperiod of 12:12 h was implemented during the experiments. Indeed, during the 12 h of light, light reactions of photosynthesis take place leading single cells mass to increase while, during the dark period, cell mass growth is inhibited and mass loss phenomena, including cell respiration, lysis, and apoptosis, prevail thus provoking a slight decrease of biomass concentration. On the other hand, it is important to highlight here that cell division takes place during night. Therefore, even the dark phase represents a crucial step of this technology.

To evaluate the applicability of *in-situ* Mars resources utilization, a further experiment was performed by replacing 20 %v/v of Z-medium volume with a corresponding value of MM. In this case, the biomass and pH evolution in time increased (Fig. 2b) without a significant lag-phase thus demonstrating that the MM components do not show an inhibiting effect on *Synechococcus* spp. Cells. The results were like those ones obtained when only Z-medium was used as growth medium, except for a slightly lower biomass concentration and a lower pH achieved at the end of the cultivation period. The replacement of 20% of Z-medium with a corresponding volume of MM did not significantly affect microalgae growth. This strategy might allow to reduce the payload associated to the nutrients needed to produce the Z-medium. As it can be seen from

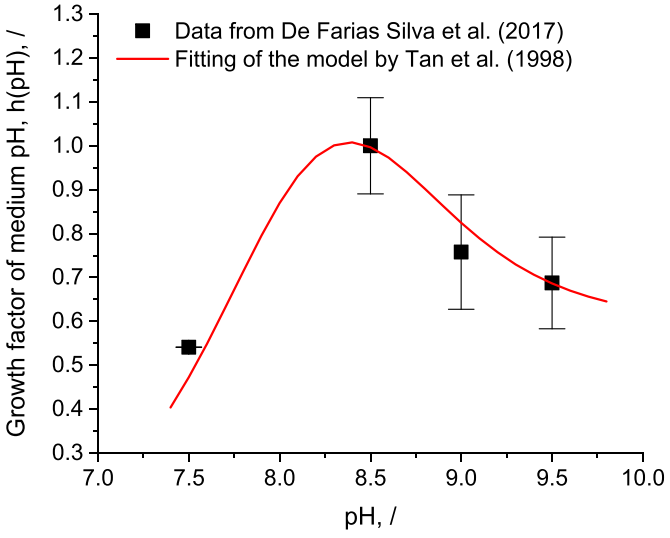

Fig. 3. Effect of pH on the controlling function h (pH) and fitting with kinetics data from literature [29].

Table 8
Parameter values obtained by fitting the experimental data by De Farias et al. [37]with the kinetics proposed by Tan et al. [33].

Parameter	Estimated value	Unit
k_0	6.0×10^{-1}	hr^{-1}
k_1	1.80	hr^{-1}
K_1	4.00×10^{-9}	$mol\ L^{-1}$
k_2	5.00×10^{-2}	hr^{-1}
K_2	9.95×10^{-9}	$mol\ L^{-1}$

Table 9
Model parameters.

Parameter	Value	Units	Reference
H_{CO_2}	8.32×10^{-1}	/	[34]
I_0	2.00×10^{1}	$\mu E\ m^{-2} s^{-1}$	Experimentally set value
$I_{K,h}$	2.97×10^{1}	$\mu E\ m^{-2} s^{-1}$	[38]
$I_{K,i}$	5.12×10^{1}	$\mu E\ m^{-2} s^{-1}$	[38]
$k_L a$	1.8×10^{1}	hr^{-1}	[39]
K_{TIC}	7.60×10^{-5}	$mol_C\ L^{-1}$	[40]
K_{TIN}	2.07×10^{-5}	$mol_N\ L^{-1}$	[41]
K_{TIP}	2.84×10^{-6}	$mol_P\ L^{-1}$	[42]
V_L	6.00×10^{-2}	L	Experimental value
V_R	4.00×10^{-2}	L	Experimental value
Y_{TIC}	4.10×10^{-2}	$mol_C\ g^{-1}$	Evaluated from [43,44]
Y_{TIN}	1.07×10^{-2}	$mol_N\ g^{-1}$	Evaluated from [45]
Y_{TIP}	4.27×10^{-5}	$mol_P\ g^{-1}$	This work
Y_{Alk}	3.83×10^{-2}	$mol\ g^{-1}$	This work
x_{air}	3.8×10^{-4}	/	Experimental value
μ_d	5.58×10^{-5}	hr^{-1}	[38]
μ_{max}	1.81×10^{-2}	hr^{-1}	[38]
τ_a	5.80×10^{-2}	$L\ m^{-1}\ g^{-1}$	[46]

Fig. 2b these data were well predicted by the proposed model, both in terms of biomass and pH, by using the same parameter values obtained as described earlier. The predictive capability of the model was supported by an average relative error in predicting the experimental data equal to 1.3% and a determination coefficient equal to 0.9997.

The replacement of Z-medium with 40%v/v of MM had a significant minor effect on the culture evolution (Fig. 2c) except for a barely detectable reduction of the overall growth rate and a stationary phase occurring after 238 h of cultivation. Even the pH evolution was like the one obtained in the MM-20 experiment except for the slightly lower values obtained at the end of cultivation related to a lower photosynthetic rate of the culture. The proposed model, though slightly overestimating the concentrations, sufficiently quantified the experimental data without tuning any parameter value. Indeed, the average relative error in predicting the experimental data was equal to 1.91% whereas the determination coefficient (r^2) was equal to 0.999.

In the case of a replacement of 60% *v/v* of ZM (In Fig. 2d) the overall growth rate significantly decreases to reach a final concentration (0.9 g L^{-1}) lower than that obtained with the lower ZM volume fraction adopted in this work. This difference might be due to a too high increase of the concentration of toxic metals of the MM or because of the osmotic shocks caused by the high salt concentration in the urine simulant. Also, a reduced nutrients content in the ZM might have contributed to the lower biomass concentration observed during the MM-60 trial. In contrast, the pH evolution was similar to that observed in previous experiments. In MM-60 one reported in Fig. 2d, model prediction was less accurate (r^2 equal to 0.994) and relative error is equal to 5.63%. Much of the error was due to the incorrect simulation of biomass concentration data. In particular, the model overestimated the experimental results especially in the final period of the cultivation probably because it neglected potential inhibition phenomena due to toxic metals and medium osmolarity increase. On the other hand, the model predicted the achievement of a stationary phase due to nutrients depletion, being the

latter one a plausible phenomenon contributing to the reduced biomass concentration experimentally detected. Therefore, although the use of 60%v/v MM would lead to a significant reduction of mission payload, it also would significantly reduce the edible biomass production thus hindering the goal of the technology. Ultimately, it can be stated that while the growth was quite low with all the media due to the low level of light intensity adopted, the model, which considers the effect of light, was capable of well simulate the experimental results. On the other hand, it is important to point out that, to validate the model and the identified set of parameter values, further experiments, performed at higher light intensities, should be carried out and simulated.

The effects of MM content in the growth medium on the feasibility of the process were further assessed by quantifying (Fig. 4) the biomass productivities (g $m^{-3}day^{-1}$) attained after 10 days of batch operation and comparing them with the prediction model.

Biomass productivities achieved when using pure Z-medium or MM-20 medium were close to 35 g m^{-3} day^{-1}. However, when the volume content of MM was increased to 40%, a slight decrease of biomass productivity to 30 g m^{-3} day^{-1} was observed. A further increase of MM content to 60% *v/v* led to a biomass productivity too low to sustain the astronauts needs in terms of food requirements. Apart from this last case, the biomass productivities were well simulated by the proposed model which thus demonstrates to be suitable to provide quantitative information on the feasibility of the process.

Ultimately, the growth medium MM-40 represented the best compromise between the investigated ones, since it would allow a significant reduction of the payload while ensuring a biomass productivity capable to satisfy the astronauts needs with relatively small photobioreactors.

As reported in a study by Enzing et al. on behalf of the Europen Union [47], *Synechococcus* sp. Was relevant among the cyanobacteria species for food applications and safety aspects. Indeed, no toxins are known to be produced by this strain [47] and no relevant cytotoxic properties have been reported in the literature [48,49] for a strain phylogenetically close to *S. nidulans,* i.e. *Synechococcus elongatus.* Moreover the possibility of using *S. nidulans* biomass as food supplement or food with high antioxidant power was also reported in the literature [50,51]. Therefore, the possibility to use cyanobacteria belonging to the *Synechococcus* species as a source for food production was confirmed by the literature. However, to further verify whether the composition of the produced algal biomass was suited for the astronauts' diet, the analysis of protein, carbohydrates and lipid content was performed (cf. Fig. 5) according to the procedures shown in the materials and methods.

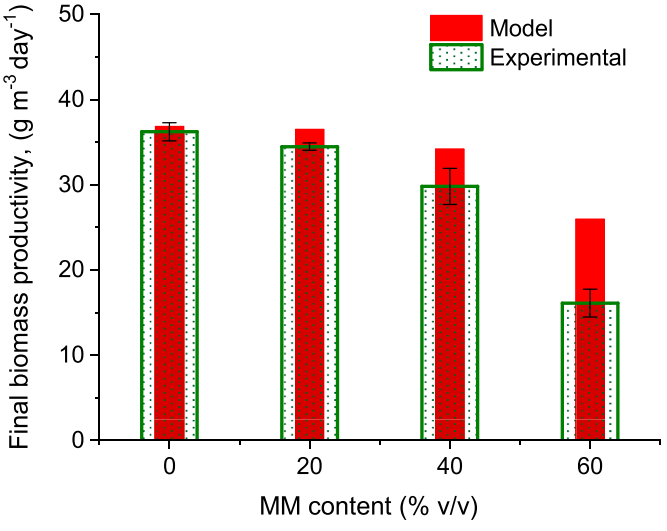

Fig. 4. Effect of MM content in the batch growth medium on the final biomass productivity after 10 days of cultivation: comparison between the biomass productivity experimental data and simulated data.

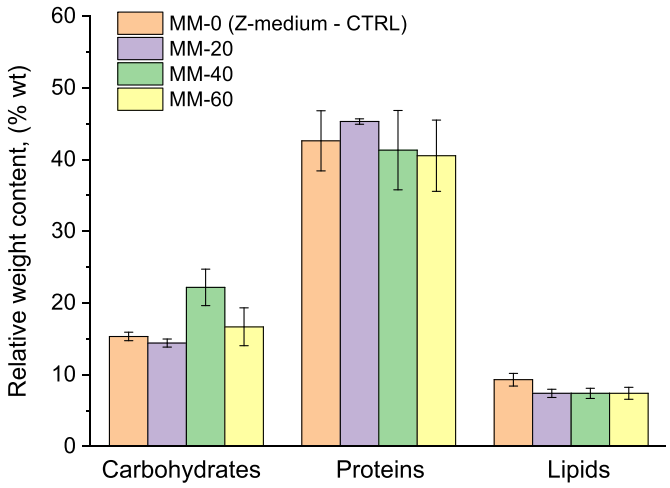

Fig. 5. Effect of growth medium composition on the content of carbohydrates, proteins and lipids in the microalgal biomass harvested at the end of cultivation (11 days).

The biomass consisted mainly of proteins (about 40 %wt) while carbohydrates and lipids were in ranges of 15–25 %wt and 7–9 %w, respectively. This composition, that well reproduces the ones reported in the literature for this strain [52], make this biomass a potential valuable source of proteins for astronauts diet. Furthermore, as it can be observed from Fig. 5, except for the case of lipids and carbohydrates in MM-40, no-significant variation of the biomass composition was observed with respect to that obtained by growing the algae in Z-medium, thus demonstrating that the use of *in-situ* available resources simulants would not result in a relevant effect on the nutritional characteristics of produced biomass.

The possibility of *S. nidulans* biomass as a food source for astronauts has been further investigated through a trolox equivalent antioxidant capacity (TEAC) assay for the analysis of its antioxidant capacity. Indeed, the exposure to ionizing radiation and reduced gravity during missions in the deep space can cause excessive production of reactive oxygen species (ROS) that contributes to cellular stress and damage in astronauts [53]. Therefore, a balanced diet rich in antioxidants is crucial for the wealthiness of astronauts. The antioxidant capacity of *S. nidulans* grown in Z-medium and MM40 measured through the TEAC assay was

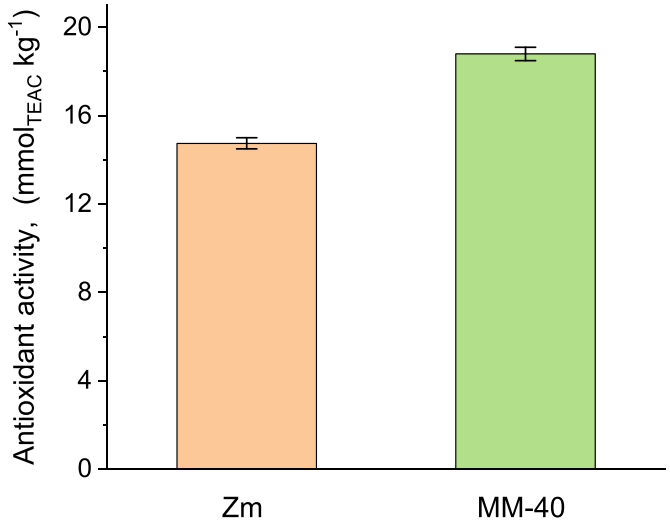

Fig. 6. Comparison between antioxidant activity of *S. nidulans* cultivated in Z-medium and MM-40 (after 11 days).

shown in Fig. 6.

Radical scavenging capacities equal ranging from 15 to 20 $mmol_{TEAC}$ kg^{-1} were obtained for the biomass grown in Z-medium and MM-40, respectively. Such values were comparable to those (~20 $mmol_{TEAC}$ kg^{-1}) reported by Goiris et al. [54] in a survey of the antioxidant capacity of different microalgal strains. Moreover, the cultivation in MM-40 led to an antioxidant power 33% higher than that one obtained with the Z-medium. This could be due to the stress provoked by the relatively high salinity and heavy metal concentration in the MM-40 which in turn may have boosted the biosynthesis of antioxidant compounds such as carotenoids. Indeed, it is well known that microalgal cells synthesize antioxidant molecules when subjected to stress conditions [55]. Thus, albeit the biochemical phenomena underlying this result should be further investigated, the phenomenological evidence showed that the use of the Martian medium led to an amelioration of the antioxidant properties of the biomass produced with the Mars media.

Some microalgal pigments such as lutein, carotenoids and phycocyanin play a key role in the diet of astronauts since they show health benefits such as anti-inflammatory, immunomodulatory, neuroprotective, hepatoprotective effects among others [56]. For this reason, the pigment content of the microalgal biomass has been quantified and shown in Fig. 7.

It can be noted that in general the use of MM-40 led to a slight decrease of the pigment content except for the case of chlorophyll and carotenoids. The increase of carotenoids content obtained with MM-40 is a welcome effect because they have relevant antioxidant and anti-inflammatory properties [57]. However, the differences between the results obtained in Z-medium and in MM-40 are not statistically relevant.

Ultimately, both literature and the biochemical characterization carried out in this work confirm that the biomass produced by cultivating *S. nidulans* in a medium produced using simulants of resources available on Mars is qualitatively suited to contribute to the feeding of astronauts in the framework of long period manned mission in the deep space.

As far as the quantitative aspects, the proposed model was adopted to predict the biomass productivity achievable on Mars. Such a prediction was performed based on the following considerations. As shown in the graphical abstract the algae could be grown in a pressurized dome wherein an atmosphere rich in CO_2 can be created by taking advantage of the Martian atmosphere. The use of Martian CO_2 would reduce the need to carry carbon sources from Earth and thus mission payload. Moreover, up to a certain concentration the increase of CO_2 content in the gas is capable to boost microalgae growth and thus biomass productivity. The photosynthetically active radiation (PAR) available on Mars changes depending upon the latitude and the season being considered while it is generally enough to promote photosynthesis of microalgae [58]. Moreover, the light within the dome can be suitably modulated by using lamps as shown in the graphical abstract. Thus, the set of values of CO_2 concentration and light intensity that maximize biomass productivity could be identified on Mars. Specifically, we have run the model for different values of light intensity and CO_2 concentration within the dome. The MM-40 medium was considered in the simulations. These results were summarized in Fig. 8 where it is seen that the better productivity was obtained for all the couples of values of light intensity and CO_2 concentration falling in the red zone.

However, to maximize the utilization of local resources the highest CO_2 concentration should be used. Therefore, the best operating condition on Mars consists of a CO_2 concentration equal to about 3 %vol and a corresponding light intensity of about 50 μE m^{-2} s^{-1}. For this reason, when applying the technique on Mars, the outdoor CO_2 should be mixed with an inert gas such as N_2 or Ar, to produce a gas mixture with 3% CO_2 before it can be insufflated and pressurized within the dome wherein algae cultivated. It is apparent that N_2 or Ar could be brought from Earth and could be continuously recycled. Under this condition, a biomass productivity of about 33 g m^{-3} day^{-1} would be obtained according to model prediction. Higher CO_2 concentration would result in a too low pH value that inhibits microalgae growth while high light intensities (at the fixed CO_2 concentration) would lead to the occurrence of photoinhibition phenomena. It should be noted that the simulation in Fig. 8 involved light intensities values of light intensities and CO_2 concentration not experimentally investigated. Therefore, the results in Fig. 8, so far discussed, should be considered a theoretical insight that should be experimentally validated before being suitably exploited.

By using the highest biomass productivity obtained in this work further evaluations have been made regarding the possibility to meet astronauts' food needs. In particular, the volumes of *S. nidulans* culture were quantified (Table 10) to meet the needs of a crew of 6 astronauts. Furthermore, it was reported the nutritional needs observed on the ISS [59] and the average composition of *S. nidulans* in Fig. 5. It should be highlighted that for these calculations, the conditions and parameters obtained with the MM-40 have been used.

Even considering a diet consisting of only of *S. nidulans*, relatively small volumes of cultures should be cultivated. In particular, to meet the protein needs of astronauts, about 34 m^3 of culture would be enough

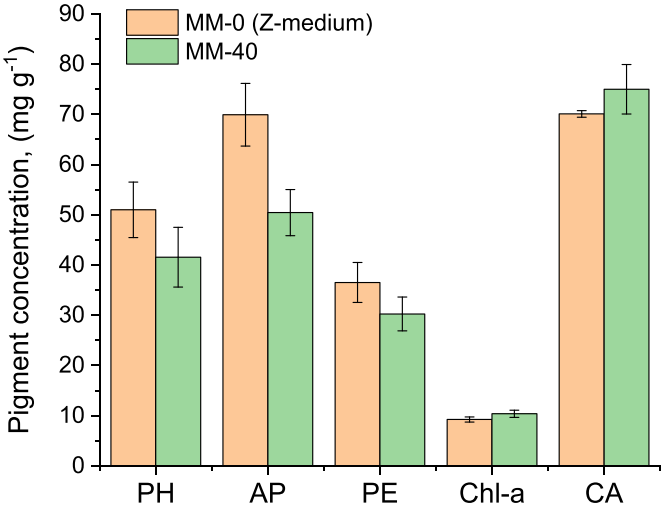

Fig. 7. Comparison between pigment compositions of *S. nidulans* cultivated in Z-medium and MM-40. PH – phycocyanin; AP – allophycocyanin; PE – phycoerythrin; Chl-a – chlorophyll-a; CA – carotenoids.

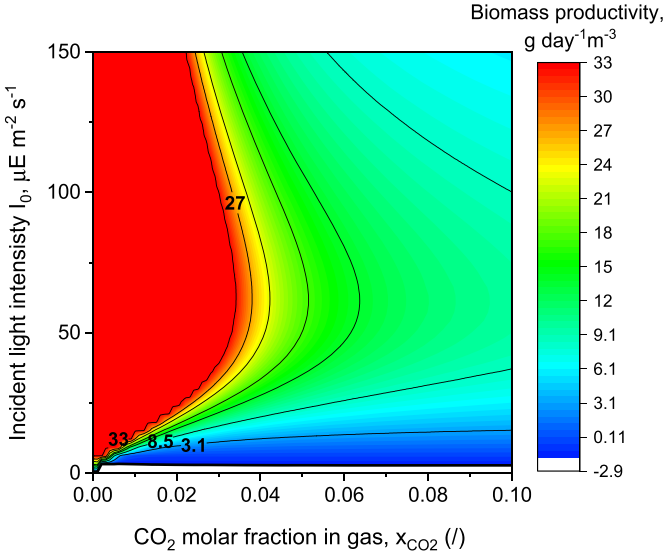

Fig. 8. Simulated effect of CO_2 concentration and light intensity on the biomass productivity of *S. nidulans* in MM-40 medium after 11 days of cultivation.

Table 10
Evaluation of the volumes of culture needed to meet the nutritional needs of a crew of 6 astronauts. The astronaut's weight is 75 kg.

Nutrient	Nutrient's need per astronaut [a] ($g\ man^{-1}\ day^{-1}$)	Nutrient's needs ($g\ kg^{-1}\ day^{-1}$)	Daily amount of nutrient needed for 6 astronauts ($g\ day^{-1}$)	Average Nutrient's content in S. nidulans[b] ($g\ g^{-1}$)	Biomass produced to meet astronauts needs ($g\ day^{-1}$)	Volume of culture to meet crew member needs[c] (m^3)
Protein	78	1.04	468	0.413	1133	34.3
Carbohydrates	58.4	0.78	350.4	0.222	1578	47.8
Lipids	64.4	0.86	386.4	0.074	5222	158.2

[a] From Bychkov et al. [59].
[b] Results obtained in this work with MM-40.
[c] Minimum volume of photobioreactors.

while the carbohydrates needs might be reached using larger volumes. If we then consider that a diet consisting only of *S. nidulans* is not feasible, the volumes of necessary culture further decreases. For instance, if we assume to satisfy 40% of the crew protein needs with *S. nidulans*, only 14 m^3 of culture would be necessary. However, it should be stressed here that such conclusions, based on modeling inferences, should be further corroborated by new experimental results before being exploited to design the photobioreactors.

The geometry and set-up of photobioreactors wherein performing cultivation could be different while in principle growth might be carried out also in specific open ponds system realized indoor within pressurized domes according to the process proposed in the patent by Cao et al. [16]. In this way the *in-situ* realization of the culture would consist of digging the regolith up to a deep of about 30–40 cm and then lining the soil with an impermeable material. To ensure a culture volume of 34 m^3 an area of about 85 m^2 would be enough. Movement of the liquid could be ensured by a pump that recirculates continuously the culture. It should be noted that, when considering the same culture volume, such a design, if compared with the ones based on the use of closed photobioreactors, would for sure result in a lower payload since it would basically consist of the liner and the pump. On the other hand, closed photobioreactors would permit to achieve higher biomass concentration and avoid contamination phenomena. Therefore, a dedicated analysis should be performed to identify the most suitable cultivation system.

Finally, it should be noted here that during its growth *S. nidulans* also produces useful O_2 which could be recovered and used to cover a specific percentage of the oxygen needs of crew members. While this aspect has not been discussed in this work it is certainly a relevant advantage of this technology that will be addressed in the future research activity.

5. Conclusions

The possibility of growing *S. nidulans* in a medium obtained by exploiting regolith leachate and urine simulant was investigated. The strain was capable to grow in media containing Martian Medium percent volumes equal to 20%v and 40%v. On the contrary when using 60%v of Martian Medium the growth rate was significantly reduced probably due to osmotic effects and too high concentration of some heavy metals from the regolith leachate. Accordingly, to minimize the amount of nutrients from Earth, the use of 40% of Martian Medium might represent the better compromise. The biochemical macro-composition of the obtained biomass showed a prevalence of proteins (~40%) followed by carbohydrates and lipids (~15–20 %wt and 7–8 %wt, respectively). Suh a composition, which might be suited to obtain food for astronauts, was not significantly affected using MM in the growth medium. This fact, together with the high content of valuable pigments such as carotenoids and the good antioxidant power, makes this strain a potential candidate for the provision of functional food to astronauts during long period missions on Mars where the sustainment is based on the use of local resources. The results of proposed mathematical model to simulate the growth of microalgae were in agreement with the experimental data obtained when using the different compositions of the growth medium. The model was then used to extrapolate the operating conditions to be set in a pressurized dome on Mars so that biomass productivities could be maximized. By taking advantage of these extrapolations along with obtained experimental data, it has been estimated that a relatively small culture volume might be enough to produce the amounts of biomass needed to stratify a significant percentage the astronaut needs in terms of proteins. However, it should be noted that such conclusions, based on modeling inferences, should be further corroborated by new experimental results before being exploited to design the photobioreactors. The envisioned cultivation system to be realized on Mars might be relatively simple and associated to small payloads. While the latter considerations should be further confirmed by additional investigations, these preliminary results indicate that the envisioned process might represent a promising approach to sustain the astronauts needs on Mars.

Declaration of competing interest

The authors declare that they have no known competing financial interests or personal relationships that could have appeared to influence the work reported in this paper.

6. Appendix 1

The concentration of total inorganic carbon in the liquid phase could be evaluated as:

$$[C_{TIC}] = [CO_{2,L}] + [H_2CO_3] + [HCO_3^-] + [CO_3^{2-}] \quad (A1)$$

The system of algebraic equations deriving by mass action law of equilibria (E1- E4) in Table 6 was formulated to express the concentrations of ionic species in solution as a function of $[H^+]$, and total inorganic carbon $[C_{TIC}]$ as follows:

$$[HCO_3^-] = K_{1C}K_C[H^+][C_{TIC}] / \psi([H^+]) \quad (A2)$$

$$[CO_3^{2-}] = K_{2C}K_{1C}K_C[C_{TIC}] / \psi([H^+]) \quad (A3)$$

$$[H_2CO_3] = K_C[H^+]^2[C_{TIC}] / \psi([H^+]) \quad (A4)$$

$$[CO_{2,L}] = [H^+]^2[C_{TIC}] / \psi([H^+]) \quad (A5)$$

where:

$$\psi([H^+]) = [H^+]^2 + K_C[H^+]^2 + K_{1C}K_C[H^+] + K_{2C}K_{1C}K \tag{A6}$$

Thus, given a specific pH value Eq. (A6) represented the required relationship between CO_2 and total inorganic carbon C_{TIC} in the liquid phase. The pH evolution was evaluated based on the electro-neutrality condition:

$$[H^+] + \sum_{i=1}^{n_{cations}} \chi_i [Cat_i^{\chi_i+}] = [OH^-] + \sum_{j=1}^{n_{anions}} \alpha_j [Ani_i^{\alpha_j-}] \tag{A7}$$

Among all the ions in Eq. (A7), only carbonates and bicarbonates are affected by the mass transfer of CO_2 from the gas phase while the remaining ones are consumed because of microalgae uptake. Thus, for each of the non-carbon ionic species reported in Eq. (A7) it can be reasonably assumed that, in a timescale greater than the one needed to achieve equilibrium, their consumption is linked to microalgae growth through a differential equation of the following type:

$$\frac{d[Ani_j^{\alpha_j-}]}{dt} = -Y_{Ani_j^{\alpha_j-}} \frac{dC_X}{dt} \quad \text{with} \quad j = 1...n_{anions} \quad \text{and} \quad Ani_j^{\alpha_j-} \neq HCO_3^-, CO_3^{2-} \tag{A8}$$

for anions and,

$$\frac{d[Cat_i^{\chi_i+}]}{dt} = -Y_{Cat_i^{\chi_i+}} \frac{dC_X}{dt} \quad \text{with} \quad i = 1...n_{cations} \tag{A9}$$

for cations. The symbols $Y_{Ani_j^{\alpha_j-}}$ or $Y_{Cat_i^{\chi_i+}}$ represent the ionic yields, i.e., the weight of biomass produced per mole of anion or cation consumed, respectively. Subsequently, in Eq. (A7) all the non-carbon ions can be grouped within a suitable term indicated with the symbol Alk:

$$[Alk] = \sum_{j=1}^{n_{anions}} \alpha_j [Ani_j^{\alpha_j-}] - \sum_{i=1}^{n_{cations}} \chi_i [Cat_i^{\chi_i+}] \quad \text{with} \quad Ani_j^{\alpha_j-} \neq HCO_3^-, CO_3^{2-} \tag{A10}$$

The latter one permits to re-write the electro-neutrality condition in Eq. (A10) in the following form:

$$[H^+] = [OH^-] + [HCO_3^-] + 2[CO_3^{2-}] + [Alk] \tag{A11}$$

Since the electro-neutrality condition should be satisfied, the kinetic evolution of *Alk* can be evaluated by considering the time derivative of *Alk*, which, considering Eq (A8, (A9) and (A10), can be evaluated as follows:

$$\frac{d[Alk]}{dt} = -\sum_{j=1}^{n_{anions}} \alpha_j Y_{Ani_i^{\alpha_j-}} \frac{dC_X}{dt} + \sum_{i=1}^{n_{cations}} \chi_i Y_{Cat_i^{\chi_i+}} \frac{dC_X}{dt} = \left(\sum_{i=1}^{n_{cations}} \chi_i Y_{Cat_i^{\chi_i+}} - \sum_{j=1}^{n_{anions}} \alpha_j Y_{Ani_i^{\alpha_j-}} \right) \cdot \frac{dC_X}{dt} \tag{A12}$$

Since all terms within parenthesis in Eq. (A12) remain constants as time changes, they can be combined in a single term Y_{alk}, and thus:

$$\frac{d[Alk]}{dt} = Y_{Alk} \frac{dC_X}{dt} \tag{A13}$$

The latter one allows evaluating [Alk] and providing the corresponding value in the electro-neutrality equation which, after inserting the expressions of Equations (A5) and (A6) of the main text and evaluating OH^- as a function of H^+, assumes the form shown in Equation (19) reported in the manuscript:

$$[H^+] = \frac{K_W}{[H^+]} + K_{1C}K_C \frac{[H^+][C_{TIC}]}{\psi([H^+])} + 2K_{2C}K_{1C}K_C \frac{[C_{TIC}]}{\psi([H^+])} + [Alk] \tag{A14}$$

which is equivalent to Equation (10) of the main text.

Notations

$\boldsymbol{a}$	Gas–liquid interfacial area $m^2\ m^{-3}$
$[\boldsymbol{Alk}]$	Sum of concentration of non-carbon ions in electro-neutrality equation mole L^{-1}
$[\boldsymbol{Ani}]$	Generic anion molar concentration mole L^{-1}
$[\boldsymbol{Cat}]$	Generic cation molar concentration mole L^{-1}
$\boldsymbol{X}$	Concentration of non lipidic microalgal biomass g L^{-1}
$[\boldsymbol{C_j}]$	Molar concentration of j_{th} nutrient in the medium, i.e., *TIC, TIN, TIP* mole L^{-1}
$\boldsymbol{f(S)}$	Nutrient dependent kinetics of continuous cell growth/
$\boldsymbol{g(I_{av})}$	Light dependent kinetics of continuous cell growth/
$\boldsymbol{h(pH)}$	pH dependent kinetics of continuous cell growth/
$\boldsymbol{H_{CO2}}$	Henry constant for the gas–liquid equilibrium of CO_2/
$\boldsymbol{I_{av}}$	Average photosynthetically active radiation within the culture μE $m^{-2}\ s^{-1}$
$\boldsymbol{I_0}$	Incident photosynthetically active radiation μE $m^{-2}\ s^{-1}$
$\boldsymbol{I_{Kh}}$	Half saturation constant of light dependent kinetics μE $m^{-2}\ s^{-1}$
$\boldsymbol{I_{Ki}}$	Inhibition constant of light dependent kinetics μE $m^{-2}\ s^{-1}$
$\boldsymbol{k_0}$	Parameter of the pH dependent kinetics) hr^{-1}

k_1	Parameter of the pH dependent kinetics hr^{-1}
K_1	Parameter of the pH dependent kinetics mole L^{-1}
K_{1C}	Equilibrium constant, cf. Table 7 mole L^{-1}
k_2	Parameter of the pH dependent kinetics) hr^{-1}
K_2	Parameter of the pH dependent kinetics mole L^{-1}
K_{2C}	Equilibrium constant, cf. Table 7 mole L^{-1}
$K_C^{'}$	Equilibrium constant, cf. Table 7 L $mole^{-1}$
$K_C^{''}$	Equilibrium constant, cf. Table 7 L $mole^{-1}$
K_j	Half saturation constant of limiting substrate (j = *TIC, TIN, TIP),* Fig. (5) mole L^{-1}
k_L	Gas–liquid mass transfer coefficient for CO_2 m hr^{-1}
K_W	Equilibrium constant for water dissociation mole L^{-1}
MW	Molecular weight g $mole^{-1}$
P_{air}	Inlet pressure of air Bar
R	Universal gas constant m^3 bar K^{-1} mol^{-1}
t	Time Min
T	Temperature K
TIC	Total inorganic carbon mole L^{-1}
TIN	Total inorganic nitrogen mole L^{-1}
TIP	Total inorganic phosphorus mole L^{-1}
V_R	Photobioreactor volume m^3
V_g	Gas phase volume m^3
V_L	Liquid volume m^3
x	Molar fraction/
Y_{Alk}	Alkalinity consumed/produced for unit weight of biomass produced mole g^{-1}
Y_J	Yield of the j_{th} limiting nutrient, j=*TIC, TIN, TIP* mole g^{-1}
Y_L	Rate of primary production of lipids/

Greek letters

α_i	Valence of the i-th anion /
θ	Function of light intensity /
μ_{max}	Maximum specific growth rate hr^{-1}
μ_d	Mass loss rate hr^{-1}
χ_j	Valence of the j-th cation /
ϱ	Cells density g L^{-1}
τ_a	Optical extinction coefficient for biomass, cf. Eq. (7) m^2 g^{-1}
ψ	Function of pH and equilibrium constant, see Eq. (20) /

Superscripts

0	Initial conditions /
f	Feed value /
g	Gas-phase /
L	Liquid-phase /

Subscripts

ani	Anionic species /
av	Average value /
cat	Cationic species /

Appendix A. Supplementary data

Supplementary data to this article can be found online at https://doi.org/10.1016/j.actaastro.2023.01.027.

References

[1] M. Kovic, Risks of space colonization, Futures, https://doi.org/10.1016/j.futures.2020.102638, 2021.

[2] E.D. Revellame, R. Aguda, A. Chistoserdov, D.L. Fortela, R.A. Hernandez, M. E. Zappi, Microalgae cultivation for space exploration: assessing the potential for a new generation of waste to human life-support system for long duration space travel and planetary human habitation, Algal Res. (2021), https://doi.org/10.1016/j.algal.2021.102258.

[3] A. Concas, G. Corrias, R. Orrù, R. Licheri, M. Pisu, G. Cao, Remarks on ISRU and ISFR technologies for manned missions on moon and mars, Eurasian Chem. J. 14 (2012) 243–248. http://www.scopus.com/inward/record.url?eid=2-s2.0-84874208661&partnerID=tZOtx3y1.

[4] L. Poughon, C. Laroche, C. Creuly, C.G. Dussap, C. Paille, C. Lasseur, P. Monsieurs, W. Heylen, I. Coninx, F. Mastroleo, N. Leys, Limnospira indica PCC8005 growth in photobioreactor: model and simulation of the ISS and ground experiments, Life Sci. Space Res. (2020), https://doi.org/10.1016/j.lssr.2020.03.002.

[5] L. Alemany, E. Peiro, C. Arnau, D. Garcia, L. Poughon, J.F. Cornet, C.G. Dussap, O. Gerbi, B. Lamaze, C. Lasseur, F. Godia, Continuous controlled long-term operation and modeling of a closed loop connecting an air-lift photobioreactor and an animal compartment for the development of a life support system, Biochem. Eng. J. (2019), https://doi.org/10.1016/j.bej.2019.107323.

[6] S. Belz, M. Buchert, J. Bretschneider, E. Nathanson, S. Fasoulas, Physicochemical and biological technologies for future exploration missions, Acta Astronaut. (2014), https://doi.org/10.1016/j.actaastro.2014.04.023.

[7] N. Kwon, D. Klein, Humans beyond Earth, SSRN Electron. J., 2019, https://doi.org/10.2139/ssrn.3459688.

[8] S.N. Nangle, M.Y. Wolfson, L. Hartsough, N.J. Ma, C.E. Mason, M. Merighi, V. Nathan, P.A. Silver, M. Simon, J. Swett, D.B. Thompson, M. Ziesack, The case for

biotech on Mars, Nat. Biotechnol. (2020), https://doi.org/10.1038/s41587-020-0485-4.
[9] D. Rapp, Use of Extraterrestrial Resources for Human Space Missions to Moon or Mars, 2018, https://doi.org/10.1007/978-3-319-72694-6.
[10] P. De Man, In-Situ Resource Utilization, 2019, https://doi.org/10.4018/978-1-5225-7256-5.ch013.
[11] C. Verseux, C. Heinicke, T.P. Ramalho, J. Determann, M. Duckhorn, M. Smagin, M. Avila, A low-pressure, N2/CO2 atmosphere is suitable for cyanobacterium-based life-support systems on mars, Front. Microbiol. (2021), https://doi.org/10.3389/fmicb.2021.611798.
[12] J. Schrader, M. Schilling, D. Holtmann, D. Sell, M.V. Filho, A. Marx, J.A. Vorholt, Methanol-based industrial biotechnology: current status and future perspectives of methylotrophic bacteria, Trends Biotechnol. (2009), https://doi.org/10.1016/j.tibtech.2008.10.009.
[13] K. Olsson-Francis, C.S. Cockell, Use of Cyanobacteria for In-Situ Resource Use in Space Applications, Planet, Space Sci, 2010, https://doi.org/10.1016/j.pss.2010.05.005.
[14] D. Billi, B. Gallego Fernandez, C. Fagliarone, S. Chiavarini, L.J. Rothschild, Exploiting a perchlorate-tolerant desert cyanobacterium to support bacterial growth for in situ resource utilization on Mars, Int. J. Astrobiol. (2021), https://doi.org/10.1017/S1473550420000300.
[15] A. Concas, A. Steriti, M. Pisu, G. Cao, Experimental and theoretical investigation of the effects of iron on growth and lipid synthesis of microalgae in view of their use to produce biofuels, J. Environ. Chem. Eng. 9 (2021), 105349, https://doi.org/10.1016/j.jece.2021.105349.
[16] Giacomo Cao, Concas Alessandro, Fais Giacomo, Gabrielli Gilberto, Manca Alessia, Pantaleo Antonella, Process and Kit to Investigate Microgravity Effect on Animal/vegetable Cells under Extraterrestrial Cultivation Conditions and Cultivation Process Thereof to Sustain Manned Space Missions, PCT/IB2012/053754, 2021.
[17] G.H. Peters, W. Abbey, G.H. Bearman, G.S. Mungas, J.A. Smith, R.C. Anderson, S. Douglas, L.W. Beegle, Mojave Mars simulant-Characterization of a new geologic Mars analog, Icarus 197 (2008) 470–479, https://doi.org/10.1016/j.icarus.2008.05.004.
[18] N. Sarigul, F. Korkmaz, İ. Kurultak, A new artificial urine protocol to better imitate human urine, Sci. Rep. 9 (2019) 1–11, https://doi.org/10.1038/s41598-019-56693-4.
[19] M. Dubois, K.A. Gilles, J.K. Hamilton, P.A. Rebers, F. Smith, Colorimetric method for determination of sugars and related substances, Anal. Chem. (1956), https://doi.org/10.1021/ac60111a017.
[20] Y. Chen, S. Vaidyanathan, Simultaneous assay of pigments, carbohydrates, proteins and lipids in microalgae, Anal. Chim. Acta (2013), https://doi.org/10.1016/j.aca.2013.03.005.
[21] E.G. Bligh, W.J. Dyer, A rapid method of total lipid extraction and purification, Can. J. Biochem. Physiol. (1959), https://doi.org/10.1139/o59-099.
[22] S.K. Mishra, W.I. Suh, W. Farooq, M. Moon, A. Shrivastav, M.S. Park, J.-W. W. Yang, Rapid quantification of microalgal lipids in aqueous medium by a simple colorimetric method, Bioresour. Technol. 155 (2014) 330–333, https://doi.org/10.1016/j.biortech.2013.12.077.
[23] O.H. Lowry, N.J. Rosebrough, A.L. Farr, R.J. Randall, Protein measurement with the Folin phenol reagent, J. Biol. Chem. (1951), https://doi.org/10.1016/s0021-9258(19)52451-6.
[24] W. Brand-Williams, M.E. Cuvelier, C. Berset, Use of a free radical method to evaluate antioxidant activity, LWT–Food Sci. Technol. (1995), https://doi.org/10.1016/S0023-6438(95)80008-5.
[25] T. Zavrel, M. Sinetova, J. Cerven, Measurement of Chlorophyll a and Carotenoids Concentration in Cyanobacteria, BIO-PROTOCOL, 2015, https://doi.org/10.21769/bioprotoc.1467.
[26] R.J. Ritchie, Consistent sets of spectrophotometric chlorophyll equations for acetone, methanol and ethanol solvents, Photosynth. Res. (2006), https://doi.org/10.1007/s11120-006-9065-9.
[27] A.R. Wellburn, The spectral determination of chlorophylls a and b, as well as total carotenoids, using various solvents with spectrophotometers of different resolution, J. Plant Physiol. (1994), https://doi.org/10.1016/S0176-1617(11)81192-2.
[28] A. Concas, G.A. Lutzu, N. Turgut Dunford, Experiments and modeling of Komvophoron sp. Growth in hydraulic fracturing wastewater, Chem. Eng. J. (2021), https://doi.org/10.1016/j.cej.2021.131299.
[29] S. Soru, V. Malavasi, A. Concas, P. Caboni, G. Cao, Modeling and experimental investigation of the effect of nitrogen starvation and pH variation on the cultivation of the extremophile microalga Coccomyxa melkonianii SCCA048, Chem. Eng. Trans. 74 (2019), https://doi.org/10.3303/CET1974033.
[30] E.M. Grima, F.G. Camacho, J.A.S. Pérez, J.M.F. Sevilla, F.G.A. Fernández, A. C. Gómez, A mathematical model of microalgal growth in light-limited chemostat culture, J. Chem. Technol. Biotechnol. 61 (1994) 167–173, https://doi.org/10.1002/jctb.280610212.
[31] E.M. Grima, F.G. Camacho, J.A.S. Pérez, F.G.A. Fernández, J.M.F. Sevilla, Evaluation of photosynthetic efficiency in microalgal cultures using averaged irradiance, Enzym. Microb. Technol. 21 (1997) 375–381.
[32] S. Soru, V. Malavasi, P. Caboni, A. Concas, G. Cao, Behavior of the extremophile green alga Coccomyxa melkonianii SCCA 048 in terms of lipids production and morphology at different pH values, Extremophiles 23 (2019) 79–89, https://doi.org/10.1007/s00792-018-1062-3.
[33] Y. Tan, Z.-X. Wang, K.C. Marshall, others, Modeling pH effects on microbial growth: a statistical thermodynamic approach, Biotechnol. Bioeng. 59 (1998) 724–731.
[34] A. Concas, , G.A.G.A.G.A. Lutzu, M. Pisu, G. Cao, Experimental analysis and novel modeling of semi-batch photobioreactors operated with Chlorella vulgaris and fed with 100%(v/v) CO 2, Chem. Eng. J. 213 (2012) 203–213, https://doi.org/10.1016/j.cej.2012.09.119.
[35] M. Marsullo, A. Mian, A.V. Ensinas, G. Manente, A. Lazzaretto, F. Marechal, Dynamic modeling of the microalgae cultivation phase for energy production in open raceway ponds and flat panel photobioreactors, Front. Energy Res. 3 (2015) 41, https://doi.org/10.3389/fenrg.2015.00041.
[36] P. Darvehei, P.A. Bahri, N.R. Moheimani, Model Development for the Growth of Microalgae: A Review, Pergamon, 2018, https://doi.org/10.1016/j.rser.2018.08.027.
[37] C.E. De Farias Silva, E. Sforza, A. Bertucco, Effects of pH and carbon source on Synechococcus PCC 7002 cultivation: biomass and carbohydrate production with different strategies for pH control, Appl. Biochem. Biotechnol. (2017), https://doi.org/10.1007/s12010-016-2241-2.
[38] A.M. Zenooz, F.Z. Ashtiani, R. Ranjbar, N. Javadi, Synechococcus sp. (PTCC 6021) cultivation under different light irradiances—modeling of growth rate-light response, Prep. Biochem. Biotechnol. (2015), https://doi.org/10.1080/10826068.2015.1084931.
[39] M. Ndiaye, E. Gadoin, C. Gentric, CO2 gas–liquid mass transfer and kLa estimation: numerical investigation in the context of airlift photobioreactor scale-up, Chem. Eng. Res. Des. (2018), https://doi.org/10.1016/j.cherd.2018.03.001.
[40] B.T. Nguyen, B.E. Rittmann, Effects of inorganic carbon and pH on growth kinetics of Synechocystis sp. PCC 6803, Algal Res. (2016), https://doi.org/10.1016/j.algal.2016.03.011.
[41] X. Tan, H. Gu, Y. Ruan, J. Zhong, K. Parajuli, J. Hu, Effects of nitrogen on interspecific competition between two cell-size cyanobacteria: microcystis aeruginosa and Synechococcus sp, Harmful Algae (2019), https://doi.org/10.1016/j.hal.2019.101661.
[42] X. Tan, H. Gu, X. Zhang, K. Parajuli, Z. Duan, Effects of phosphorus on interspecific competition between two cell-size cyanobacteria: Synechococcus sp. and microcystis aeruginosa, Bull. Environ. Contam. Toxicol. (2019), https://doi.org/10.1007/s00128-018-2527-x.
[43] Y. Chisti, Biodiesel from microalgae, Biotechnol. Adv. 25 (2007) 294–306, https://doi.org/10.1016/j.biotechadv.2007.02.001.
[44] E.P. Bennion, D.M. Ginosar, J. Moses, F. Agblevor, J.C. Quinn, Lifecycle assessment of microalgae to biofuel: comparison of thermochemical processing pathways, Appl. Energy 154 (2015) 1062–1071, https://doi.org/10.1016/J.APENERGY.2014.12.009.
[45] M.C. Picardo, J.L. de Medeiros, J.G.M. Monteiro, R.M. Chaloub, M. Giordano, O. de Q.F. Araújo, A methodology for screening of microalgae as a decision making tool for energy and green chemical process applications, Clean Technol. Environ. Policy 15 (2013) 275–291.
[46] C. Jeffryes, J. Rosenberger, G.L. Rorrer, Fed-batch cultivation and bioprocess modeling of Cyclotella sp. for enhanced fatty acid production by controlled silicon limitation, Algal Res. 2 (2013) 16–27, https://doi.org/10.1016/j.algal.2012.11.002.
[47] C. Enzing, M. Ploeg, M. Barbosa, L. Sijtsma, Microalgae-based products for the food and feed sector: an outlook for Europe, JRC Sci. Policy Reports (2014), https://doi.org/10.2791/3339.
[48] K. Hayashi, T. Hayashi, I. Kojima, A natural sulfated polysaccharide, calcium spirulan, isolated from Spirulina platensis: in vitro and ex vivo evaluation of anti-herpes simplex virus and anti-human immunodeficiency virus activities, AIDS Res. Hum. Retrovir. (1996), https://doi.org/10.1089/aid.1996.12.1463.
[49] Y.Y. Kok, W.L. Chu, S.M. Phang, S.M. Mohamed, R. Naidu, P.J. Lai, S.N. Ling, J. W. Mak, P.K.C. Lim, P. Balraj, A.S.B. Khoo, Inhibitory Activities of Microalgal Extracts against Epstein-Barr Virus DNA Release from Lymphoblastoid Cells, J. Zhejiang Univ. Sci. B., 2011, https://doi.org/10.1631/jzus.B1000336.
[50] S. Gunes, S. Tamburaci, E. Imamoglu, M.C. Dalay, Determination of superoxide dismutase activities in different cyanobacteria for scavenging of reactive oxygen species, J. Biol. Act. Prod. from Nat. (2015), https://doi.org/10.1080/22311866.2014.983973.
[51] L.S. Fanka, G.M. da Rosa, M.G. de Morais, J.A.V. Costa, Outdoor production of biomass and biomolecules by spirulina (arthrospira) and Synechococcus cultivated with reduced nutrient supply, Bioenergy Res (2021), https://doi.org/10.1007/s12155-021-10320-1.
[52] J.H. Duarte, J.A.V. Costa, Synechococcus nidulans from a thermoelectric coal power plant as a potential CO2 mitigation in culture medium containing flue gas wastes, Bioresour. Technol. (2017), https://doi.org/10.1016/j.biortech.2017.05.064.
[53] X. Gómez, S. Sanon, K. Zambrano, S. Asquel, M. Bassantes, J.E. Morales, G. Otáñez, C. Pomaquero, S. Villarroel, A. Zurita, C. Calvache, K. Celi, T. Contreras, D. Corrales, M.B. Naciph, J. Peña, A. Caicedo, Key Points for the Development of Antioxidant Cocktails to Prevent Cellular Stress and Damage Caused by Reactive Oxygen Species (ROS) during Manned Space Missions, Npj Microgravity, 2021, https://doi.org/10.1038/s41526-021-00162-8.
[54] K. Goiris, K. Muylaert, I. Fraeye, I. Foubert, J. De Brabanter, L. De Cooman, Antioxidant potential of microalgae in relation to their phenolic and carotenoid content, J. Appl. Phycol. (2012), https://doi.org/10.1007/s10811-012-9804-6.
[55] C. Faraloni, G. Torzillo, Synthesis of antioxidant carotenoids in microalgae in response to physiological stress, Carotenoids (2017), https://doi.org/10.5772/67843.
[56] T.J. Ashaolu, K. Samborska, C.C. Lee, M. Tomas, E. Capanoglu, Ö. Tarhan, B. Taze, S.M. Jafari, Phycocyanin, a super functional ingredient from algae; properties, purification characterization, and applications, Int. J. Biol. Macromol. (2021), https://doi.org/10.1016/j.ijbiomac.2021.11.064.

[57] J. Ávila-Román, S. Garc\'\ia-Gil, A. Rodr\'\iguez-Luna, V. Motilva, E. Talero, Anti-inflammatory and anticancer effects of microalgal carotenoids, Mar. Drugs 19 (2021) 531.
[58] N.S. Kruyer, M.J. Realff, W. Sun, C.L. Genzale, P. Peralta-Yahya, Designing the bioproduction of Martian rocket propellant via a biotechnology-enabled in situ resource utilization strategy, Nat. Commun. 12 (2021) 6166, https://doi.org/10.1038/s41467-021-26393-7.
[59] A. Bychkov, P. Reshetnikova, E. Bychkova, E. Podgorbunskikh, V. Koptev, The current state and future trends of space nutrition from a perspective of astronauts' physiology, Int. J. Gastron. Food Sci. (2021), https://doi.org/10.1016/j.ijgfs.2021.100324.